

## Strengthening contributions in ultra-high strength cryorolled Al–4%Cu–3%TiB<sub>2</sub> in situ composite

N. NAGA KRISHNA, K. SIVAPRASAD, P. SUSILA

Advanced Materials Processing Laboratory, Department of Metallurgical and Materials Engineering,  
National Institute of Technology, Tiruchirappalli, Tamil Nadu 620015, India

Received 13 June 2013; accepted 26 August 2013

**Abstract:** Ultra-high strength Al alloy system was developed by cryorolling and the contribution of various strengthening mechanisms to the overall yield strength of the system was evaluated. Cryorolling of Al–4%Cu–3%TiB<sub>2</sub> in situ composite followed by short annealing at 175 °C and ageing at 125 °C resulted in an ultra-high yield strength of about 800 MPa with 9% total elongation. The strengthening contributions from solid solution strengthening, grain refinement, dislocation strengthening, precipitation hardening and dispersion strengthening were evaluated using standard equations. It was estimated that the maximum contribution was from grain refinement due to cryorolling followed by precipitation and dispersion strengthening.

**Key words:** Al alloy; cryorolling; metal matrix composites; ultrafine grained microstructure; strengthening mechanisms

### 1 Introduction

Cryorolling is a unique mechanical deformation process at cryogenic temperature by which high strength and ductility combinations can be achieved. This combination of properties was attributed to a bimodal grain size distribution with micrometer sized grains embedded inside the matrix of nano/ultrafine grain (UFG) microstructure [1]. The UFG imparts high strength as expected from the Hall–Petch relationship, whereas the micrometer sized grains contribute to the enhancement of ductility [2]. The suppression of dynamic recovery during deformation at cryogenic temperature preserves a high density of defects generated by deformation, which can act as the potential recrystallization sites. Accordingly, the cryogenic deformation would require less plastic deformation for achieving UFG structure, compared to the severe plastic deformation processes at ambient or elevated temperatures [3].

In the present work, the microstructure and mechanical properties of cryorolled (CR) Al–4%Cu alloy and Al–4%Cu–3%TiB<sub>2</sub> in situ composite were investigated. In situ composites are multiphase materials where the reinforcement is developed within the matrix

during the composite fabrication preferably by casting route. In situ composites are preferred over the ex situ composites because of the tailorable size of reinforcing particles, clean interface between matrix and dispersoids and economy in processing [4]. The reinforced TiB<sub>2</sub> particles of the Al–4%Cu–3%TiB<sub>2</sub> in situ composite resulted in high yield strength in tension with reasonably good elongation. Similar results were reported by other investigators in which the tensile properties and aging kinetics of the in situ composites were enhanced [5,6]. Many reports are available on cryorolling of different aluminum alloys [7–9] and in situ composites [5,10]. However, no published work is available in assessing the role of different strengthening mechanisms. Hence, the present investigation makes an attempt to evaluate the contribution from various strengthening mechanisms to the overall room temperature tensile yield strength for the CR alloy as well as the in situ composite and these results are compared with the experimental values. The contribution to strengthening will be due to a combination of five individual mechanisms. While the mechanism of strengthening by a reduction in grain size takes place via the Hall–Petch effect, the in situ particles will strengthen the alloy through Orowan mechanism and the solute will enhance the strength by solid solution strengthening. Apart from these, the other components of

strengthening that will be operative are dislocation strengthening attained due to sub-zero deformation and precipitation hardening attained due to aging treatment. Thus the role of different strengthening mechanisms in such UFG materials and the relative extent to which each mechanism contributes to the overall strength is analyzed.

## 2 Experimental

Al–4%Cu alloy was used as the base metal and two types of salts, viz., potassium hexafluorotitanate ( $K_2TiF_6$ ) and potassium tetrafluoroborate ( $KBF_4$ ), were used to synthesize the  $TiB_2$  reinforcement. The alloy was melted at 850 °C in the muffle furnace and the salts were pre-heated to 250 °C for 1 h, and by the stirring method, the pre-heated salts were slowly added into the molten Al alloy in an atomic ratio in accordance with Ti/2B. The in situ  $TiB_2$  particles were formed by the chemical reactions between the two salts and the molten Al alloy. After specified reaction time, the composite was degassed and cast into rectangular plates of 130 mm×130 mm×7 mm. The cast alloy plates were solutionized at 500 °C for 1 h and quenched in chilled water. The solutionized plates were dipped in a liquid propanol bath maintained at –80 °C for about 1 h. Then the plates were rolled from 7 mm thickness to 0.25 mm thickness and the total thickness reduction of 96% was achieved in multiple passes with about 5% reduction per pass. After each pass, the plates were immersed in liquid propanol again for 5 min before further reduction. Later the cryorolled sheets were subjected to short time annealing (3 min) at 175 °C. Aging treatment was performed for 8 h at 125 °C. X-ray diffraction (XRD) analysis was carried out using Rigaku Ultima III XRD unit (with a Cu  $K_\alpha$  radiation of 1.5406 Å). Tensile tests were carried out on the alloy and on the composite both in as-CR condition and in as-CR condition followed by short annealing (SA) and aged condition. All the tensile tests were performed at room temperature on standard sub-size specimens with Instron tensile testing unit (table top model). To study the dislocation structure and precipitation, Philips CM20 transmission electron microscope (TEM) was used.

## 3 Results and discussion

Figure 1 shows the XRD pattern of the cast and solutionized in situ composite, which indicates the presence of  $TiB_2$  and  $Al_2Cu$  peaks. The field-emission scanning electron micrograph of the composite shown in Fig. 2(a) reveals the hexagonal shaped  $TiB_2$  particles and also a clean interface between the matrix and the reinforcement. The corresponding EDS pattern is

indicated in Fig. 2(b), with the most intense peak in the pattern corresponding to Al, which is the matrix and the remaining peaks show the presence of Ti and B. This clearly evidences that these hexagonal shaped particles are  $TiB_2$ . TEM bright field images for different processing conditions are indicated in Fig. 3, which contains dark regions with large dislocation density along with large dislocation tangles. Region A in Fig. 3(a)

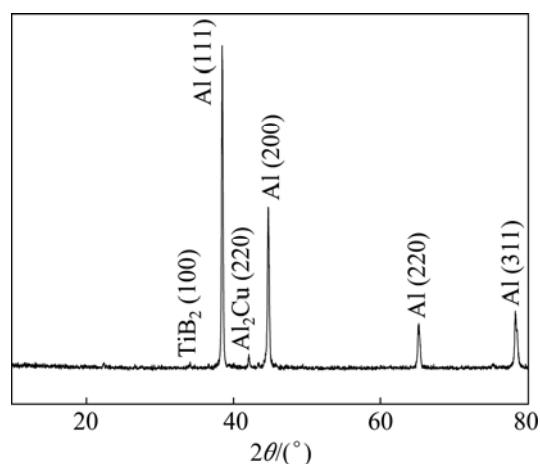


Fig. 1 X-ray diffractogram of cast and solutionized in situ composite

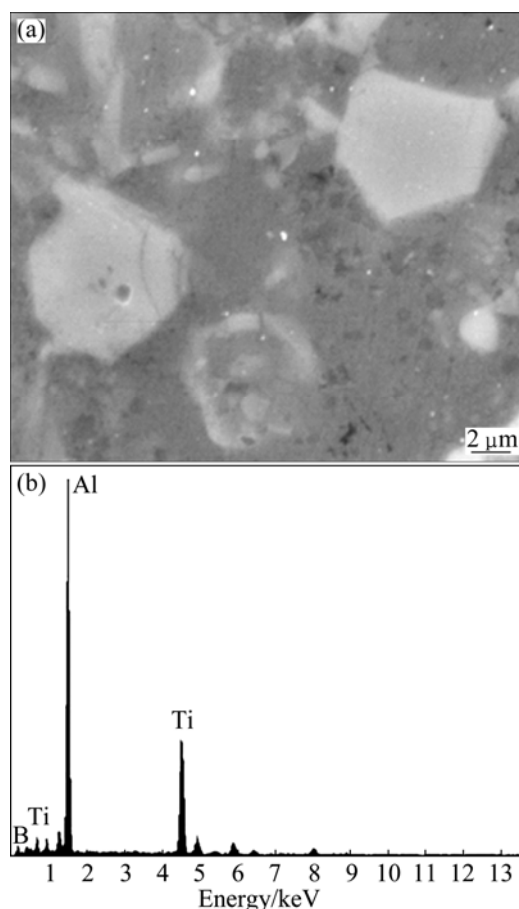
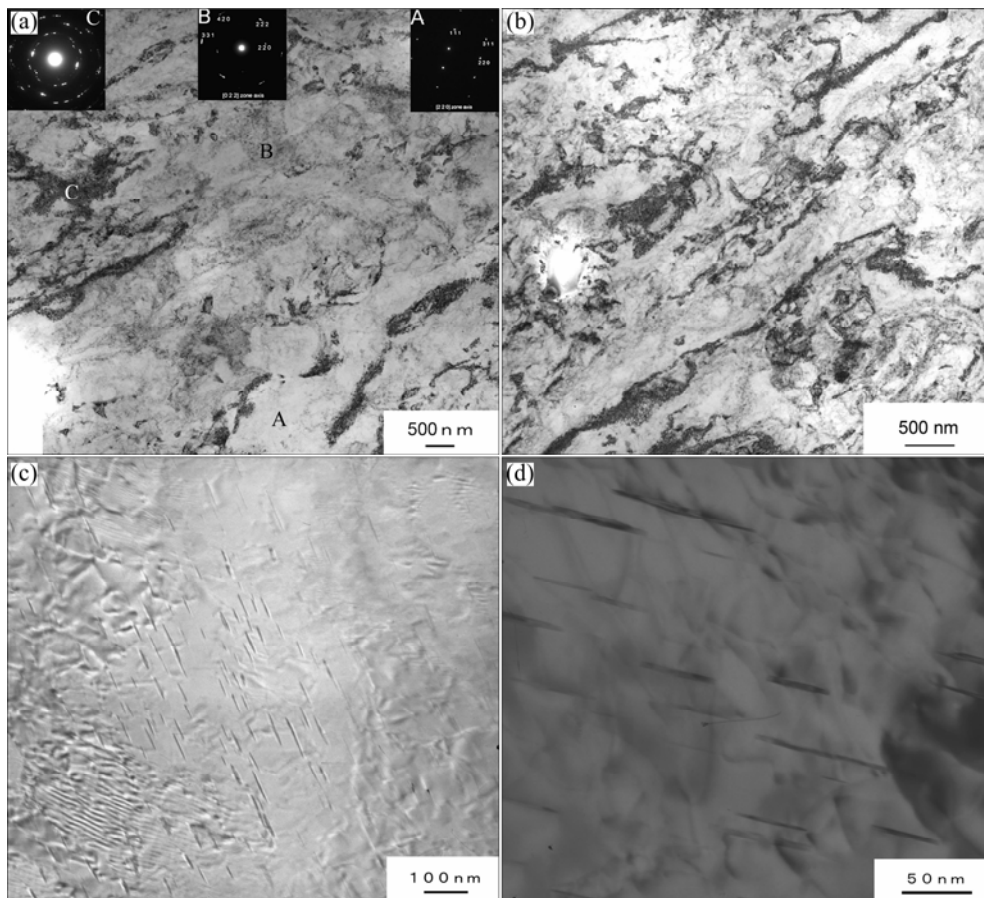


Fig. 2 SEM image (a) of in situ composite and corresponding EDS pattern (b)

indicates the presence of coarse grains which are evidenced by spot pattern of the selected area electron diffraction (SAED) pattern. Similarly, fine grains are observed to be present in region B which is revealed from the ring pattern, while region C contains UFG/nano structure evidenced from ring pattern of SAED. Hence the structure consists of both coarse grains as well as UFG/nano structure. Figure 3(b) indicates more amount of dislocation density in the case of composite in as-CR condition compared with the CR base alloy. The

presence of  $\text{TiB}_2$  dispersions could have acted as a barrier for the dislocation movement and it can be observed from Table 1 that the contribution of dislocation hardening was more in as-CR composite (114 MPa) whereas for CR alloy it was 103 MPa. Figure 3(c) corresponds to the microstructure in peak aged condition showing needle-like precipitates and the observed precipitates are intermediate phases  $\theta''$  or  $\theta'$ , while Fig. 3(d) shows the presence of dispersoid as well as the precipitates. The maximum strengthening was achieved



**Fig. 3** TEM bright field images: (a) Al-4%Cu alloy in as-CR condition; (b) Al-4%Cu-3TiB<sub>2</sub> in situ composite in as-CR condition; (c) Al-4%Cu alloy in CR condition, SA at 175 °C (3 min) and aging at 125 °C for 8 h; (d) Al-4%Cu-3TiB<sub>2</sub> in situ composite in CR condition, SA at 175 °C (3 min) and aging at 125 °C for 8 h

**Table 1** Contribution to total yield strength from various strengthening mechanisms for 0.2% proof stress

Alloy	Solid solution $\sigma_0$ /MPa	Grain refinement $\sigma_{gs}$ /MPa	Dislocation $\sigma_{dis}$ /MPa	Precipitate $\sigma_{ppt}$ /MPa	Dispersoid $\sigma_{dispersoid}$ /MPa	RMS summation/MPa	Experimental strength/MPa	Elongation/%
As-CR alloy	90	428	103	–	–	530	533	8
CR-SA alloy	90	409	79	–	–	507	522	11
CR-SA-aged alloy	37	379	42	249	–	492	616	8
As-CR composite	90	473	114	–	262	643	699	7
CR-SA composite	90	448	82	–	262	615	673	7
CR-SA-aged composite	37	406	68	263	262	591	800	9

in the case of composite in aged condition, which is mainly attributed to strengthening from precipitation and from dispersions.

The contribution from different strengthening mechanisms to the total yield strength is indicated in Table 1 and it can be observed that, the composite in CR-SA and aged condition exhibited yield strength and elongation of 800 MPa and 9%, respectively. Thus the major advantage of this route is that the ultra-high strength is achieved without losing ductility. In order to tailor the microstructure–property correlation, it would be interesting to understand the contribution of individual strengthening mechanism to the overall yield strength. Hence the current attempt is to identify the contribution of several strengthening mechanisms to the overall yield strength based on theoretical analysis. The following strengthening mechanisms were evaluated by using theoretical formulae.

### 3.1 Solid solution strengthening

The alloy consists of 4% Cu in Al in solid solution, which can contribute a significant strength to the alloy. This can be assessed by using an equation proposed by TELLKAMP et al [11]. Equation (1) indicates the increase in strength due to the addition of copper as solid solution hardener strengthener.

$$\sigma_0 = \sigma_{\text{pure}} + HC^n \quad (1)$$

where  $\sigma_{\text{pure}}$  is the flow stress for the pure Al which is about 35 MPa;  $H$  is the increase in strength of Al through addition of Cu per mass which is 13.8 MPa [12];  $C$  is the Cu content in mass fraction and  $n=1$ . The above equation can be rewritten as

$$\sigma_0 = \sigma_{\text{pure}} + 13.8 C \quad (2)$$

The maximum strengthening due to 4% Cu in Al is ~55 MPa. Thus the strength due to solid solution is 90 MPa. The mechanism of solid solution strengthening involves an increase in tensile strength and yield stress

produced by alloying elements in solid solution. The elements in the solution produce elastic distortions in the parent lattice thereby acting as a barrier to dislocation movements with Cu being considered as one of the prominent solutes for solid solution hardening [13]. However, in the aged condition, majority of Cu takes part in precipitation with Al and only 0.13% Cu [14] contributes to the solid solution strengthening at room temperature (~2 MPa). As indicated in Table 1, in the aged condition, the contribution of solid solution strengthening is 37 MPa.

### 3.2 Grain refinement

Apart from solid solution strengthening, strengthening due to grain refinement has significant contribution to overall strength achieved by the system. The increase in yield strength due to grain refinement can be obtained by the Hall–Petch relation and is given as

$$\sigma_{\text{gs}} = \sigma_0 + K_y d^{-\frac{1}{2}} \quad (3)$$

where  $\sigma_0$  is given by equation (2);  $K_y$  is the Hall–Petch constant which is given as 0.1 to 0.2 MN/m<sup>3/2</sup> [15] and  $d$  is the grain size. Based on the modified Voigt function [16], the crystallite size was measured with the instrumental broadening being taken care using standard Al sample. The alloy in as-CR condition resulted in a crystallite size of around 169 nm (as indicated in Table 2) and in SA, SA and aged condition it is around 188 nm and 226 nm respectively. The increase in crystallite size in the latter conditions is associated with the phenomenon of recrystallization and grain growth. In the case of composite processed in all the three conditions, a further reduction in grain size enabled higher yield strength.

Similar results were reported by ZHAO et al [17] in which a yield strength of 650 MPa was achieved in the

**Table 2** Parameters related to strengthening mechanisms

Processing condition	Dislocation density/m <sup>-2</sup>	Crystallite size/nm	Inter-precipitate spacing ( $L_0$ )/nm	Thickness of precipitate ( $t$ )/nm	Inter-particle spacing between dispersoids ( $L$ )/ $\mu\text{m}$	Average radius of dispersoids ( $r$ )/ $\mu\text{m}$
As-CR Al–4%Cu	$2.2 \times 10^{14}$	169				
CR-SA Al–4%Cu	$1.3 \times 10^{14}$	188				
CR-SA-aged Al–4%Cu	$3.6 \times 10^{13}$	226	38	4		
As-CR composite	$2.7 \times 10^{14}$	134			114	13
CR-SA composite	$1.4 \times 10^{14}$	152	36	4	114	13
CR-SA-aged composite	$9.7 \times 10^{13}$	191			114	13

case of a combination of equal-channel-angular pressing (ECAP) by route B<sub>C</sub> and natural aging process for a 7075 Al alloy. However, in the present investigation, the cryorolled Al–4%Cu alloy in the SA and aged condition achieved a yield strength of 379 MPa. The enhanced yield strength exhibited by 7075 Al alloy may be attributed to the high strain that is induced by the ECAP process. In a similar manner, a maximum value of 473 MPa grain size strengthening was achieved in a as-CR composite. SHANMUGASUNDARAM et al [18] reported a strength of 692 MPa due to grain refinement in a bulk nanostructured Al–4Cu alloy which was produced by mechanical alloying followed by vacuum hot pressing. The variation in the contribution may be due to the nanostructured grains (in the order of 50 nm) that were achieved after ball milling and vacuum hot pressing, while cryorolling process resulted in an average grain size of 134 nm. As reported elsewhere [19], after nine ECAP passes of AA2014 in T6 condition, the grain size was refined from 50 μm to 3 μm and the corresponding yield strength was 230 MPa. However, in the present investigation, the process of cryorolling resulted in UFG/nano structure, with which a higher yield strength of 409 MPa was achieved.

### 3.3 Dislocation hardening

As the alloy is subjected to severe plastic deformation, a large amount of dislocation pile-up was observed. An increase in dislocation density leads to an increase in strength and is given by the following relation [20]:

$$\sigma_{\text{dis}} = \alpha M G b \sqrt{\rho} \quad (4)$$

where  $\alpha$  is a constant varying from 0.2 to 0.3;  $G$  is the shear modulus of Al which is 27 GPa;  $b$  is the Burgers vector (for Al  $b=0.286$  nm);  $M$  is the Taylor factor (for randomly oriented FCC polycrystals it is  $\sim 3$ );  $\rho$  is the dislocation density. Based on X-ray diffraction peak profile analysis, the dislocation density was calculated which is indicated in Table 2 for different processing conditions. The dislocation density was measured based on the following equation [16]:

$$\rho = \frac{2\sqrt{3} \langle \varepsilon^2 \rangle^{\frac{1}{2}}}{Db} \quad (5)$$

where  $\varepsilon$  is the RMS microstrain and  $D$  is the average crystallite size obtained from XRD analysis. The crystallite size was measured by modified Voigt function [16]. From Table 1, it can be seen that the contribution of dislocation hardening to the overall strength in the case of as-CR alloy is 103 MPa, whereas in the SA, SA and aged condition, the contribution is 79 MPa and 42 MPa respectively. Compared with SA treatment conditions,

as-cryorolled condition exhibited superior strength, which may be attributed to high dislocations in its structure in as-CR form. In SA condition, the contribution of dislocation hardening was reduced by about 23% compared with as-CR condition which is due to annihilation of dislocations due to the thermal energy supplied during short annealing. A dislocation strengthening of about 42 MPa was observed in the SA and aged condition, which is due to further reduction in the dislocation density due to aging process. In the case of composite, fine dispersoids impede the dislocation movement and thus a higher value of dislocation hardening was obtained compared with the alloy processed under similar conditions.

### 3.4 Precipitation hardening

The major strengthening mechanism generally observed in age hardenable alloys is due to precipitation. Moreover, the severe plastic deformation enhances the precipitation kinetics of these alloys. Hence, the precipitation hardening is calculated as suggested by GILMORE and STARKE [21]. The increase in critical resolved shear stress due to distribution of plate-shaped precipitates on a specific set of planes is given by the following equation [20].

$$\Delta\tau = \frac{Gb}{2\pi\sqrt{1-\nu}} \left( \frac{1}{L_o} \right) \ln \left( \frac{At}{r_o} \right) \quad (6)$$

Multiplying the above equation with Taylor factor, the contribution from precipitates to the flow stress can be obtained as follows:

$$\sigma_{\text{ppt}} = \frac{M G b}{2\pi\sqrt{1-\nu}} \left( \frac{1}{L_o} \right) \ln \left( \frac{At}{r_o} \right) \quad (7)$$

where  $\nu$  is the Poisson ratio ( $\sim 0.3$ );  $L_o$  is the inter-precipitate spacing;  $A$  is the geometric parameter related to habit planes of the precipitates (for  $\{1\ 0\ 0\}$  it is 1.225);  $t$  is the thickness of the precipitate;  $r_o$  is equivalent to  $2b$ . The CR alloy in the SA and aged condition resulted in precipitation strengthening of 255 MPa which is due to enhanced precipitation kinetics due to the accumulation of high stored energy during cryorolling. However, an increased strengthening of 265 MPa was observed in the case of composite processed in the same condition which is attributed to the presence of dispersoids.

### 3.5 Dispersion strengthening

As the alloy is reinforced with TiB<sub>2</sub> particles, it is also necessary to calculate the strength contribution from dispersion strengthening. The influence of nano-sized dispersoids on the resolved shear stress is given as follows [22]:

$$\tau_b \cong \frac{Gb}{L-2r} \quad (8)$$

Equation (9) indicates the contribution from dispersoids to the flow stress.

$$\sigma_{\text{dispersoid}} = \frac{MGB}{L-2r} \quad (9)$$

where  $L$  is the inter particle spacing and  $r$  is the particle size. Table 1 shows the dispersoid strengthening of 262 MPa for all the composites processed in the mentioned conditions. This is based on the assumption that the dispersoid size and distribution do not vary too much during SA and aging process.

The contribution to the total strength (0.2% proof stress) from the various sources is given in Table 1. Although the summation of components of strength has usually been linear, a number of researchers have considered the root mean square (RMS) summation to be more appropriate [23]. It is evident from Table 1 that the experimental values are in close approximation to the RMS summation values.

RMS summation  $\sigma_y$  can be written as follows:

$$\sigma_y = \sigma_0 + (\sigma_{\text{gs}}^2 + \sigma_{\text{dis}}^2 + \sigma_{\text{ppt}}^2 + \sigma_{\text{dispersoid}}^2)^{1/2} \quad (10)$$

Figure 4 indicates the individual contributions in various conditions of cryorolled sheets. It is evident that grain refinement is the major contributor to the total strength, followed by precipitation and dispersion strengthening.

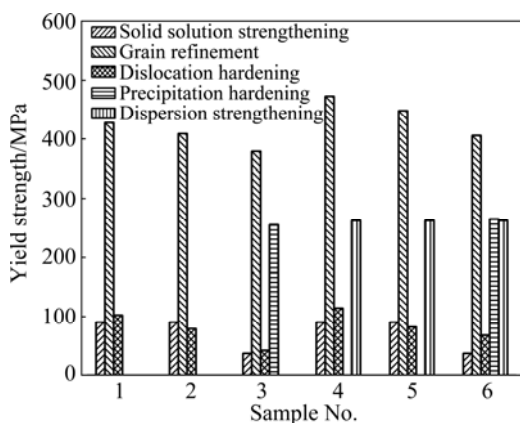


**Fig. 4** Histogram showing contributions of various strengthening mechanisms to strength of samples: 1—Al-4%Cu in as-CR condition; 2—Al-4%Cu in CR-SA condition at 175 °C (3 min); 3—Al-4%Cu in CR-SA condition at 175 °C (3 min), aged at 125 °C (8 h); 4—Composite in as CR condition; 5—Composite in CR-SA condition at 175 °C (3 min); 6—Composite in CR-SA condition at 175 °C (3 min), aged at 125 °C (8 h)

## 4 Conclusions

Cryorolling of in situ composite resulted in

combinations of ultra-high strength and elongation, strengthening contributions like solid solution, grain refinement, dislocation, precipitation and dispersion strengthening mechanisms were evaluated. In the case of cryorolled composite subjected to SA and aging, grain refinement contributed ~51% followed by precipitation and dispersion strengthening and the remaining from others mechanisms. Grain refinement and dislocation strengthening were observed to be more in as-CR condition of both alloy and composite than in SA or aged condition, which may be attributed to thermal relaxation and partial recrystallization.

## Acknowledgements

The authors gratefully acknowledge the Department of Science & Technology (DST) for their financial support for carrying out this research through Fast Track Scheme (DST Sanction No: SR/FT/ET-005/2008) and Technical Education Quality Improvement Programme (TEQIP). The authors also thank Prof. K. HONO and Dr. T. T. SASAKI of NIMS, Japan for extending their help in TEM.

## References

- [1] WANG Y, CHEN M, ZHOU F, MA E. High tensile ductility in a nanostructured metal [J]. *Nature*, 2002, 419: 912–915.
- [2] GIL SEVILLANO J, ALDAZABAL J. Ductilization of nanocrystalline materials for structural applications [J]. *Scripta Materialia*, 2004, 51(8): 795–800.
- [3] RANGARAJU N, RAGHURAM T, VAMSI KRISHNA B, PRASAD RAO K, VENUGOPAL P. Effect of cryo-rolling and annealing on microstructure and properties of commercially pure aluminium [J]. *Materials Science and Engineering A*, 2005, 398(1–2): 246–251.
- [4] TJONG S C, MA Z Y. Microstructural and mechanical characteristics of in situ metal matrix composites [J]. *Materials Science and Engineering R*, 2000, 29(3–4): 49–113.
- [5] NAGA KRISHNA N, SIVAPRASAD K. High temperature tensile properties of cryorolled Al-4%Cu-3%TiB<sub>2</sub> in-situ composites [J]. *Transactions of the Indian Institute of Metals*, 2011, 64(1–2): 63–66.
- [6] MANDAL A, MAITI R, CHAKRABORTY M, MURTY B S. Effect of TiB<sub>2</sub> particles on aging response of Al-4Cu alloy [J]. *Materials Science and Engineering A*, 2004, 386(1–2): 296–300.
- [7] PANIGRAHI S K, JAYAGANTHAN R, CHAWLA V. Effect of cryorolling on microstructure of Al-Mg-Si alloy [J]. *Materials Letters*, 2008, 62(17–18): 2626–2629.
- [8] NAGA KRISHNA N, TEJAS R, SIVAPRASAD K, VENKATESWARLU K. Study on cryorolled Al-Cu alloy using X-ray diffraction line profile analysis and evaluation of strengthening mechanisms [J]. *Materials & Design*, 2013, 52: 785–790.
- [9] GOPALA KRISHNA K, SIVAPRASAD K, VENKATESWARLU K, HARI KUMAR K C. Microstructural evolution and aging behavior of cryorolled Al-4Zn-2Mg alloy [J]. *Materials Science and Engineering A*, 2012, 535: 129–135.
- [10] GOPI B, NAGA KRISHNA N, SIVAPRASAD K, VENKATESWARLU K. Effect of rolling temperature on microstructure and mechanical properties of cryorolled Al-Mg-Si alloy reinforced with 3wt% TiB<sub>2</sub> in-situ composite [J]. *Advanced Materials Research*, 2012, 584: 556–560.

- [11] TELLKAMP V L, LAVERNIA E J, MELMED A. Mechanical behavior and microstructure of a thermally stable bulk nanostructured alloy [J]. Metallurgical and Materials Transactions A, 2001, 32(9): 2335–2343.
- [12] American Society for Metals. ASM metals reference book: Volume 2 [M]. Metals Park, OH: 1979: 38.
- [13] TOTEN G E, MACKENZIE D S. Handbook of aluminium—Physical metallurgy and processes [M]. New York: Marcel Dekker, 2003: 261.
- [14] American Society for Metals. ASM metals reference book: Volume 4 [M]. Metals Park, OH: 1979: 841.
- [15] EMBURY J D. Strengthening mechanisms in Al alloys—An overview of natural limits and engineering possibilities [J]. Materials Science Forum, 1996, 217–222: 57–70.
- [16] de KEIJSER T H, LANGFORD J I, MITTEMEIJER E J, VOGELS A B P. Use of the voigt function in a single-line method for the analysis of X-ray diffraction line broadening [J]. Journal of Applied Crystallography, 1982, 15: 308–314.
- [17] ZHAO Y H, LIAO X Z, ZHU Y T, VALIEV R Z. Enhanced mechanical properties in ultrafine grained 7075 Al alloy [J]. Journal of Materials Research, 2005, 20(2): 288–291.
- [18] SHANMUGASUNDARAM T, HEILMAIER M, MURTY B S, SUBRAMANYA SARMA V. Microstructure and mechanical properties of nanostructured Al–4Cu alloy produced by mechanical alloying and vacuum hot pressing [J]. Metallurgical and Materials Transactions A, 2009, 40(12): 2798–2801.
- [19] MALLIKARJUNA C, SHASHIDHARA S M, MALLIK U S. Evaluation of grain refinement and variation in mechanical properties of equal-channel angular pressed 2014 aluminium alloy [J]. Materials & Design 2009, 30(5): 1638–1642.
- [20] TAYLOR G I. The mechanism of plastic deformation of crystals. Part I. Theoretical [J]. Proceedings of Royal Society A, 1934, 145: 362–387.
- [21] GILMORE D L, STARKE E A. Trace element effects on precipitation processes and mechanical properties in an Al–Cu–Li alloy [J]. Metallurgical and Materials Transactions A, 1997, 28(7): 1399–1415.
- [22] COURTNEY T H. Mechanical behavior of materials [M]. New Delhi: Overseas Press, 2006: 208.
- [23] IRVINE J, BAKER T N. The influence of rolling variables on the strengthening mechanisms operating in niobium steels [J]. Materials Science and Engineering, 1984, 64(1): 123–134.

## 低温轧制超高强度 Al–4%Cu–3%TiB<sub>2</sub> 原位复合材料的强化机理

N. NAGA KRISHNA, K. SIVAPRASAD, P. SUSILA

Advanced Materials Processing Laboratory, Department of Metallurgical and Materials Engineering,  
National Institute of Technology, Tiruchirappalli, Tamil Nadu 620015, India

**摘要:** 为了开发超高强度铝合金和评估各种强化机制对合金屈服强度的影响, 将 Al–4%Cu–3%TiB<sub>2</sub> 进行低温轧制, 然后再在 175 °C 下快速退火、在 125 °C 下时效。在总伸长率为 9% 的情况下, Al–4%Cu–3%TiB<sub>2</sub> 原位复合材料得到 800 MPa 的高强度。使用标准方程来评估固溶强化、晶粒细化、位错强化、弥散强化和析出硬化等各种强化机制的贡献。其中贡献最大的是低温轧制引起的晶粒细化, 其次是析出硬化、弥散强化。

**关键词:** 铝合金; 低温轧制; 金属基复合材料; 超细晶组织; 强化机理

(Edited by Hua YANG)